Available online at www.sciencedirect.com
ScienceDirect
Trans. Nonferrous Met. Soc. China 32(2022) 2587−2597
Transactions of Nonferrous Metals Society of China
www.tnmsc.cn

Effect of annealing temperature on microstructure and mechanical properties of cold-rolled commercially pure titanium sheets

Shuai ZHAO[1], Yang WANG[1], Lin PENG[1,2], Yuan-xiang ZHANG[1], Rong RAN[1], Guo YUAN[1]

1. State Key Laboratory of Rolling and Automation, Northeastern University, Shenyang 110819, China;
2. Pangang Group Research Institute Company Limited, Panzhihua 617067, China

Received 18 July 2021; accepted 8 December 2021

Abstract: The strength of traditional commercially pure titanium (CP-Ti) alloys often fails to meet the demand of structural materials. In order to enhance their mechanical properties, the cold-rolled CP-Ti alloys were annealed at different temperatures, and the recrystallization behavior and texture evolution were investigated. It was found that the bimodal microstructure (equiaxed and elongated grains) was formed after partial recrystallization, and the corresponding sample exhibited an excellent combination of ultimate tensile strength (702 MPa) and total elongation (36.4%). The recrystallization nucleation of CP-Ti sheets occurred preferentially in the high strain and the high-angle grain boundaries (HAGBs) regions. Meanwhile, the internal misorientations of the deformed heterogeneous grains increased and transformed into HAGBs, which further promoted the recrystallization nucleation. The main recrystallization texture was basal TD-split texture transformed from cold-rolled basal RD-split texture, and the oriented nucleation played a dominated role during recrystallization.

Key words: commercially pure titanium; recrystallization nucleation; bimodal microstructure; mechanical properties; texture

1 Introduction

Due to good biocompatibility, excellent corrosion resistance and high specific strength, titanium and its alloys have been widely used in medical devices, chemical equipment, aerospace and many other fields [1−4]. Unfortunately, because of few alloying elements, CP-Ti alloys cannot be strengthened. So far, severe plastic deformation (SPD) has been widely employed to improve the strength. ISLAMGALIEV et al [5] found that grain refinement of CP-Ti (from 40 μm to 105−120 nm) could be achieved by high-pressure torsion, leading to an enhanced ultimate tensile strength (about 1600 MPa) while also accompanied by the loss of elongation. According to MENG et al [6], high strain rate rotary swaging of CP-Ti brought about profuse twins and rapid grain refinement at room temperature, as a result, the ultimate tensile strength was about 976 MPa, but its elongation was less than 10%. Also, KANG and KIM [7] and NASIRI-ABARBEKOH et al [8] refined the grains of CP-Ti by multi-pass equal channel angular pressing (ECAP), indicating that ECAP can significantly improve the strength, besides, the elongation was close to 20%. The above research indicates that although SPD can refine the grain size and improve the strength, while this method often sacrifice elongation.

There is no doubt that the heat treatment process is of crucial importance for tailoring the strength-to-plastic ratio of materials. LIU et al [9] reported the effect of annealing on mechanical

Corresponding author: Yang WANG, Tel: +86-15242086602, E-mail: wangyang@ral.neu.edu.cn;
Guo YUAN, Tel: +86-13609880996, E-mail: yuanguoneural@163.com
DOI: 10.1016/S1003-6326(22)65968-5

properties of CP-Ti rods by rotary swaging and they attributed the excellent combination of strength and ductility to the ultrafine grain size and the high dislocation density in the interior of grains. GU et al [10] studied the effect of short-term annealing on the mechanical properties of bulk ultrafine-grained (UFG) pure titanium (Grade 2). It was found that UFG Ti can achieve a perfect combination of strength (R_m: 663 MPa) and good elongation (A: 29%) by short-term annealing at 300 °C for 15 min. LI et al [11] proved that selective laser melted CP-Ti annealing at 650 °C could generate the equiaxed microstructure in the acicular α' region, resulting in weakened texture. LIN et al [12] found that short-term annealing after high-pressure torsion improved the ductility of CP-Ti, but its strength would decrease at higher annealing temperatures due to grain growth. The above studies were mostly focused on the effects of grain sizes after heat treatment on properties. Moreover, it has been reported that the excellent combination of strength and plasticity was achieved by introducing multimodal grain structure in face-centered cubic metal copper [13].

Therefore, this work aimed to tailor the microstructure of cold-rolled CP-Ti sheets through recrystallization annealing. And the bimodal microstructure (equiaxed and elongated grains) was the contributor to the enhanced mechanical properties, which made it possible for CP-Ti sheets to meet the requirement of structural material. What's more, the recrystallization behavior and texture evolution during annealing were analyzed in depth.

2 Experimental

The as-received CP-Ti material was 100 mm (length) × 20 mm (width) × 2 mm (thickness) annealed sheets in this study, and its chemical composition is shown in Table 1. The CP-Ti sheets were cold rolled to 0.8 mm by multi-pass unidirectional rolling, and the total reduction was 60%. In order to study the effect of the annealing temperature on the mechanical properties, recrystallization and texture of the sheets, the sheets were annealed at 500, 550, 600 and 650 °C for 10 min in a tube furnace (argon atmosphere). The tensile specimens with dimensions of 10 mm (gauge length) × 5 mm (width) × 0.8 mm (thickness) were machined with longitudinal axis parallel to the rolling direction. The tensile samples were stretched at room temperature with a rate of 0.5 mm/min, and three tensile samples were tested under each condition. Samples were cut from the as-received and annealed sheets, and the samples were electropolished in a solution consisting of 50 mL perchloric acid, 600 mL methanol and 350 mL n-butanol at 30 V and −20 °C. Electropolishing samples were detected by electron backscattered diffraction (EBSD) technology, and the data were analyzed with the HKL Channel 5 software to obtain the grain sizes, recrystallized grains, grain boundary distribution and texture characteristics.

Table 1 Chemical composition of CP-Ti sheets (mass fraction, %)

Fe	O	N	C	H	Ti
0.12	0.15	0.008	0.03	0.005	Bal.

3 Results

3.1 As-received material

The microstructure and texture of as-received CP-Ti sheet are shown in Fig. 1. Figure 1(a) shows that the as-received CP-Ti sheet consists of fully recrystallized equiaxed grains. The average grain size is approximately 5.6 μm. Figure 1(b) shows the grain boundary distribution of the as-received sheet. Grain boundaries with misorientations lower and higher than 15° were denoted as low angle grain boundaries (LAGBs) and high angle grain boundaries (HAGBs), respectively. The as-received material had a large number of uniformly distributed HAGBs (proportion 0.776). There was a weak basal bimodal texture in the {0002} pole map of the as-received sheet, and the maximum pole density was 4.68, as shown in Fig. 1(c). The c-axis of some grains was approximately parallel to the ND, and the c-axis of other grains deflected approximately 70° along the ND to TD. The orientation of $\{10\bar{1}0\}$ pole map grains was randomly distributed.

3.2 Annealing microstructure

Band contrast maps of CP-Ti sheets annealed at different temperatures are shown in Fig. 2. With the increase of annealing temperature, the

microstructure of CP-Ti sheets transformed from deformed microstructure into bimodal microstructure (equiaxed and elongated grains), and finally into completely equiaxed microstructure. After annealing at 500 °C, cold-rolled structure still remained in the matrix (Fig. 2(a)). Elongated grains can be seen in the microstructure and the average grain size was about 1.9 μm. According to Fig. 2(b), when annealing at 550 °C, recrystallization in the large deformation regions and many fine equiaxed grains can be observed. Also, there were some deformed grains along the RD. The average grain

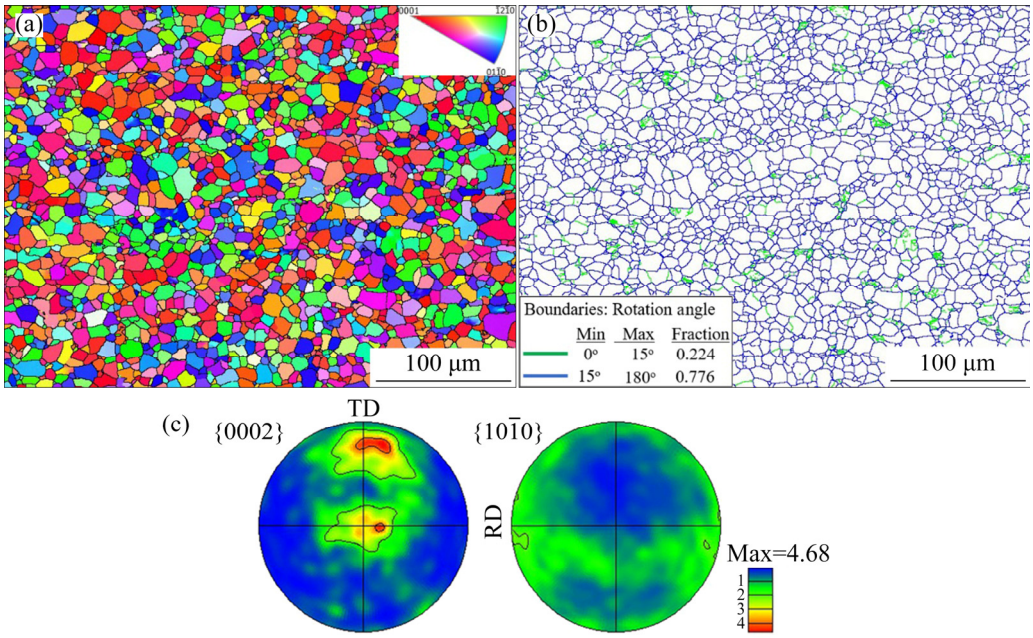

Fig. 1 IPF map (a), grain boundary distribution (b), and pole map (c) of as-received CP-Ti sheets

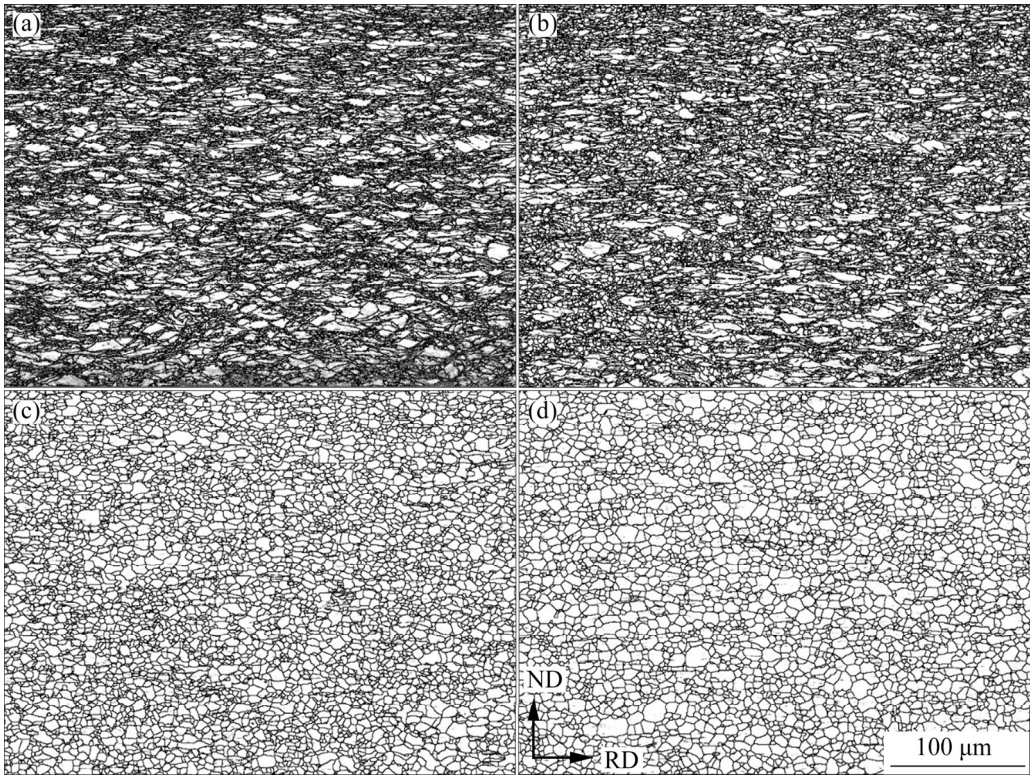

Fig. 2 Band contrast maps of CP-Ti sheets annealed at different temperatures: (a) 500 °C; (b) 550 °C; (c) 600 °C; (d) 650 °C

size was about 2.0 μm. As shown in Figs. 2(c) and (d), the microstructures of CP-Ti sheets annealed at 600 and 650 °C were all equiaxed grains, and the average grain sizes were 3.6 and 4.3 μm, respectively.

3.3 Mechanical properties

The tensile properties of different samples are presented in Fig. 3. The specific tensile properties are listed in Table 2. Obviously, the flow curves were significantly affected by annealing temperatures. It can be seen from Fig. 3 that the ultimate tensile strength (R_m: 582 MPa) of the as-received CP-Ti sheet was the lowest, but it exhibited good elongation (A: 39.5%). After cold rolling and annealing, the CP-Ti sheet after annealing at 500 °C exhibited the highest tensile strength (R_m: 754 MPa) while lower elongation (A: 29.4%). After the peak stress (ultimate tensile stress), it exhibited rapid flow softening. The excellent combination of strength and plasticity can be achieved when annealing at 550 °C, the ultimate

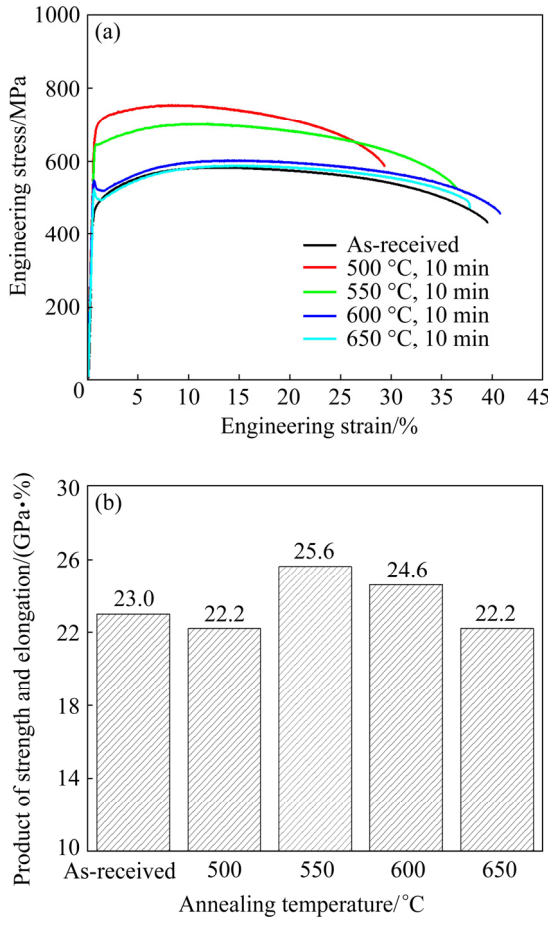

Fig. 3 Engineering stress−strain curves (a) and product of strength and elongation values (b) of CP-Ti sheets annealed at different temperatures

Table 2 Tensile strengths and product of strength and elongation values under annealing

Sample	$R_{p0.2}$/MPa	R_m/MPa	A/%	$R_m \cdot A$/(GPa·%)
As-received	463	582	39.5	23.0
500 °C, 10 min	688	754	29.4	22.2
550 °C, 10 min	645	702	36.4	25.6
600 °C, 10 min	533	602	40.8	24.6
650 °C, 10 min	506	588	37.8	22.2

tensile strength was 702 MPa, and the elongation was 36.4%. Moreover, the product of strength and elongation (25.6 GPa·%) was the highest, indicating that it had excellent strength and toughness level. For the samples annealed at 600 and 650 °C, the tensile properties were similar to that of the as-received sheet.

3.4 Recrystallized grains distribution

The recrystallized grains distribution of CP-Ti sheets after different annealing temperatures are shown in Fig. 4. As can be seen in Fig. 4, the recrystallized grains, substructured grains and deformed grains are distinguished by blue, yellow and red regions, respectively. It can be seen from Fig. 4(a) that the deformed structure accounts for the majority (proportion 0.981) of the CP-Ti plate annealed at 500 °C. Figure 4(b) shows partial recrystallization occurred in CP-Ti sheet annealed at 550 °C, a large fraction of deformed structure (proportion 0.726) still existed in the matrix, and there were also some recrystallized grains (proportion 0.267). When CP-Ti sheet was annealed at 600 °C, the microstructure was mainly composed of recrystallized grains (proportion 0.934) and a small amount of deformed matrix (proportion 0.054), as shown in Fig. 4(c). With the further increase of annealing temperature, the microstructure of CP-Ti sheet annealed at 650 °C was completely recrystallized and accompanied by grains growth. The proportion of recrystallized grains was 0.974, as shown in Fig. 4(d).

3.5 Grain boundaries distribution

Figure 5 shows the grain boundaries distribution of CP-Ti sheets annealed at different temperatures. It can be seen from Fig. 5(a) that the CP-Ti sheet annealed at 500 °C was filled with high-density LAGBs, and the proportions of

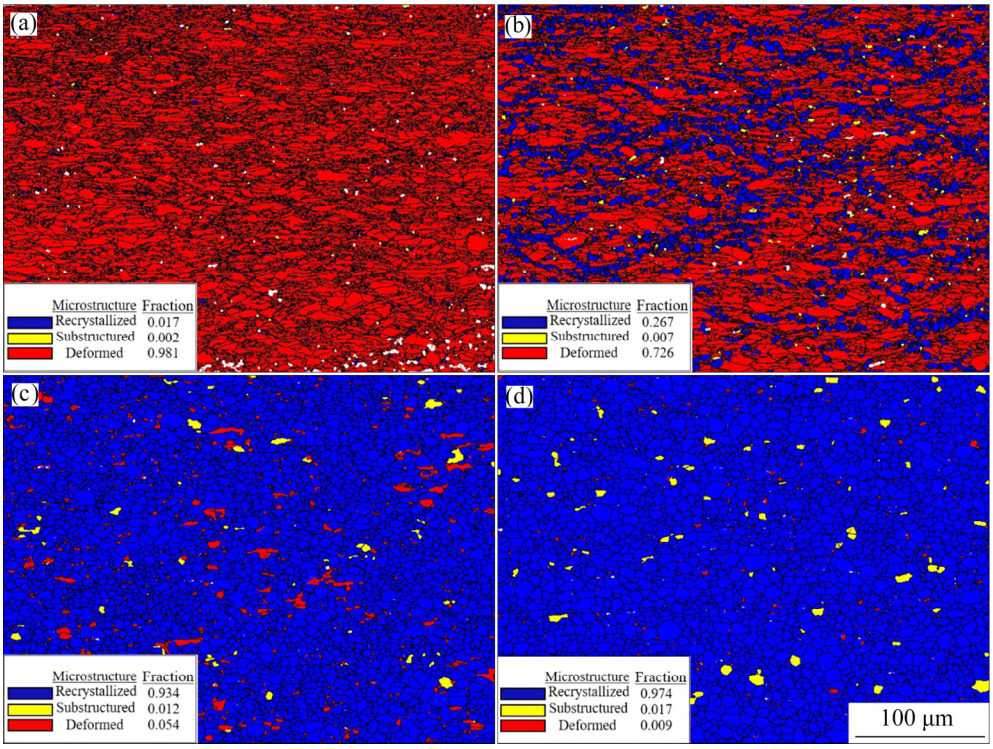

Fig. 4 Recrystallized grains distribution of CP-Ti sheets annealed at different temperatures: (a) 500 °C; (b) 550 °C; (c) 600 °C; (d) 650 °C

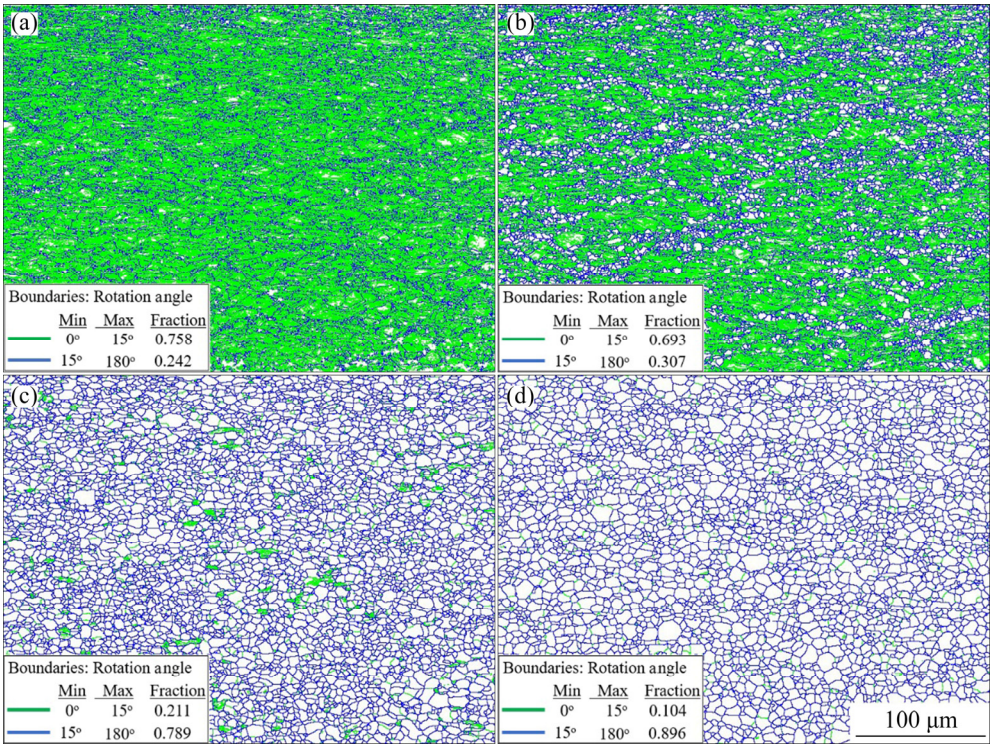

Fig. 5 Grain boundaries distribution of CP-Ti sheets annealed at different temperatures: (a) 500 °C; (b) 550 °C; (c) 600 °C; (d) 650 °C

LAGBs and HAGBs were 0.242 and 0.758, respectively. It indicated that some defects formed during the cold-rolling process still existed after the annealing treatment. When CP-Ti sheet was annealed at 550 °C, the LAGBs density decreased and many defect-free grains were generated, as

shown in Fig. 5(b). The CP-Ti sheet annealed at 600 °C was mainly composed of grains without lattice distortion, and the fraction of HAGBs increased to 0.789. In Fig. 5(d), the grains of CP-Ti sheet annealed at 650 °C were basically new grains without lattice distortion, and the HAGBs increased further, accounting for 0.896. With the increase of annealing temperature, the proportion of HAGBs increased, resulting in new grains without lattice distortion.

3.6 Pole maps and orientation distribution function

The {0002} and {10$\bar{1}$0} pole maps of CP-Ti sheets annealed at different temperatures are shown in Fig. 6. In Figs. 6(a) and (b), when CP-Ti sheets were annealed at 500 and 550 °C, there were mainly many *c*-axis orientations of grains deflected near ±20° from ND to RD. Meanwhile, the intensity in the {0002} pole maps decreased. In addition, the *c*-axis orientation of some grains deflected near 30° from ND to TD. Moreover, the intensity of CP-Ti annealed at 550 °C was slightly high, and the maximum multiple uniform distribution was 5.17. When the CP-Ti sheet was annealed at 600 °C, the *c*-axis orientation of more grains deflected from ND to TD by 40°, as shown in Fig. 6(c). When the CP-Ti sheet was annealed at 650 °C, the *c*-axis orientation of more grains deflected from ND to TD by ±35°, as shown in Fig. 6(d). With the increase of annealing temperature, the intensity of the {0002} pole map of CP-Ti sheets was weakened firstly and then was strengthened slightly. The density of {0002} pole map of the sheet annealed at 550 °C was the lowest. Interestingly, the RD-split basal texture of CP-Ti annealed sheets transformed into basal TD-split texture, and the intensity was strengthened slightly.

In order to obtain the evolution of annealing texture of CP-Ti sheets, orientation distribution function (ODF) maps were used to further characterize the texture characteristics at different annealing temperatures. The main texture orientation of CP-Ti sheets was located on the sections of Φ_2=0° and Φ_2=30°, as shown in Fig. 7. In Figs. 7(a) and (b), it can be seen that the textures of CP-Ti sheets annealed at 500 and 550 °C were both $(01\bar{1}5)[1\bar{3}21]$ and $(0001)[0\bar{3}31]$, and the texture intensity of CP-Ti sheet annealed at 550 °C was lower. When the annealing temperature rose to 600 °C, the recrystallization textures of CP-Ti sheet were $(01\bar{1}2)[3\bar{2}\bar{1}0]$ and $(11\bar{2}4)[5\bar{6}11]$, as shown in Fig. 7(c). Compared with the texture of CP-Ti sheet annealed at 600 °C, the texture orientation of CP-Ti sheet annealed at 650 °C moved about 10° to the direction of Φ=0°, and the recrystallization textures were $(01\bar{1}3)[3\bar{2}\bar{1}0]$ and $(11\bar{2}5)[4\bar{5}10]$, as shown in Fig. 7(d).

4 Discussion

4.1 Evolution of microstructure and mechanical properties

Different annealing temperatures of the CP-Ti sheets resulted in significant microstructure differences. It can be seen from Fig. 2 that as the

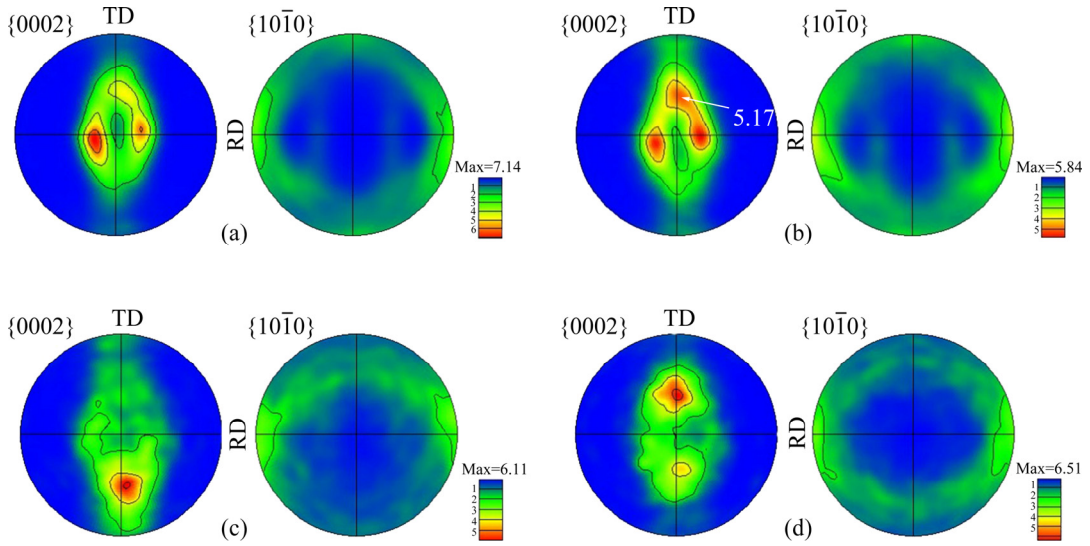

Fig. 6 Pole maps of cold-rolled CP-Ti sheets annealed at different temperatures: (a) 500 °C; (b) 550 °C; (c) 600 °C; (d) 650 °C

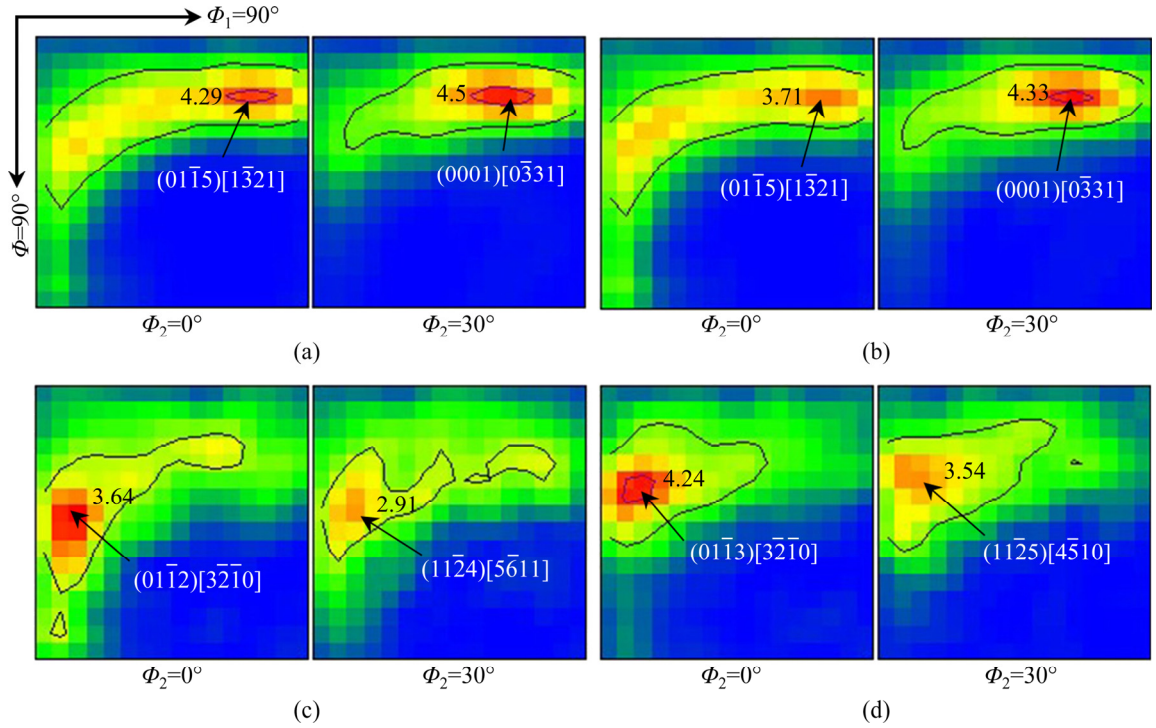

Fig. 7 ODF maps of CP-Ti sheets annealed at different temperatures: (a) 500 °C; (b) 550 °C; (c) 600 °C; (d) 650 °C

annealing temperature increased, the microstructure gradually transformed from the elongated grains into uniform equiaxed grains. The microstructure of CP-Ti sheet after annealing at 600 °C was almost equiaxed grains. In addition, it can be seen from the grain boundaries distribution (Fig. 5) that the proportion of HAGBs of CP-Ti sheets gradually increased. The main reason was the migration and aggregation of subgrain boundaries during annealing increased grain boundary misorientation angles, leading to the transition from LAGBs with higher energy to HAGBs with lower energy, which induced the formation of equiaxed grains [14−16]. The growth of grains during annealing at 650 °C can be attributed to the decrease of interfacial energy.

CP-Ti sheets exhibited different mechanical properties because of the different microstructures after annealing, as shown in Fig. 3 and Table 2. The microstructure of CP-Ti sheet annealed at 500 °C maintained the original processing morphology. Severely deformed equiaxed grains lost the ability to emit and transmit dislocations, resulting in low elongation. With the increase of annealing temperature, the ultimate tensile strength and yield strength of CP-Ti sheets gradually decreased, and the elongation increased. After reaching the peak stress, the partially recrystallized and fully recrystallized specimens of CP-Ti sheets showed gradual flow softening. The reason was that a large number of LAGBs transformed into HAGBs (Fig. 5), which reduced dislocation density of the grains and enhanced softening effect. Meanwhile, the grain boundaries of equiaxed crystals can emit and transmit dislocations, which can better coordinate plastic deformation [17]. When the specimen was annealed at 650 °C, the mechanical properties were similar to that of as-received sheet. This can be attributed to the fact that the refined grains grew up during annealing, resulting in the decrease of strength.

It can be seen from Figs. 2 and 3 that the equiaxed microstructure exhibited low strength and good ductility, while the microstructure of elongated grains along the RD exhibited high strength and low ductility. However, when the CP-Ti sheet was annealed at 550 °C, the bimodal microstructure exhibited optimal comprehensive mechanical properties, and the product of strength and elongation reached 25.6 GPa·%. Therefore, when the CP-Ti sheet was annealed at 550 °C, bimodal microstructure can be achieved through partial recrystallization, which was beneficial to obtaining an excellent combination of high strength and good plasticity.

4.2 Recrystallization behavior

As the annealing temperature increased, the proportion of recrystallized grains of the CP-Ti sheet increased. High annealing temperature accelerated the occurrence of recrystallization and generated equiaxed grains without lattice distortion. It can be found in Fig. 4(b) that recrystallization grains preferentially nucleated and grew in high strain regions. The reason was that the CP-Ti sheet had high deformation energy storage in the high strain regions, which promoted the nucleation and growth of recrystallization [18].

In addition, according to the microstructure of the annealed sheets, it can be concluded that the elongated and deformed grains along the RD direction would finally transform into equiaxed grains. In order to explore the recrystallization behavior, ten larger deformation heterogeneous grains (numbers A−J) of CP-Ti sheets were respectively selected from 500 and 550 °C annealed sheets, as shown in Fig. 8. The orientations of A−J grains of CP-Ti sheets annealed at 500 and 550 °C were similar. However, the intragranular maximum misorientation of A−J grains of CP-Ti sheet annealed at 550 °C was larger than that at 500 °C, as shown in Figs. 8(a) and (b). The maximum misorientation within A−J grains of CP-Ti sheet annealed at 550 °C was larger than 4.5° (accounting for 80%), as shown in Fig. 8(c). This indicates that the recovery degree of A−J grains of CP-Ti sheet

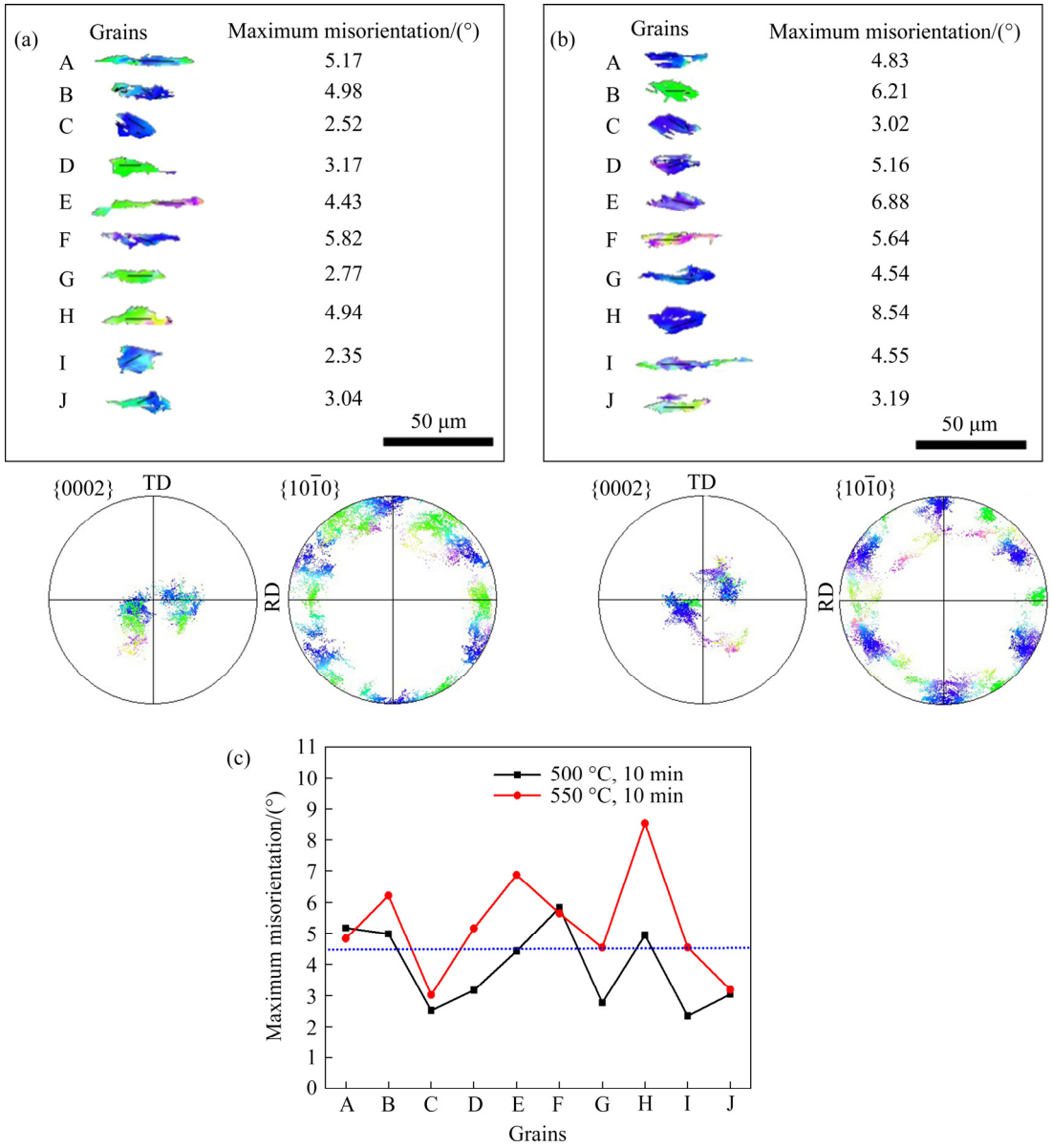

Fig. 8 Internal maximum misorientations of deformation heterogeneous grains of CP-Ti sheets annealed at 500 °C (a), 550 °C (b), and comparison of maximum misorientations in annealed samples (c)

annealed at 550 °C is great. It can also be seen from Fig. 5 that the proportion of subgrains decreased with the increase of annealing temperature. Finally, the deformation heterogeneous grains transformed into HAGBs grains. Previous studies have shown that subgrain boundaries with low mobility were converted into highly mobile HAGBs in deformation heterogeneous grains, which was believed to be a viable mechanism for nucleation of recrystallization [19−21]. Therefore, it can be inferred that during the annealing of CP-Ti sheets, recrystallization nucleation preferentially occurred in the high strain and HAGBs regions. At the same time, the subgrain boundaries in the deformation heterogeneous grains migrated and gradually transformed into HAGBs, which promoted the nucleation of recrystallization.

4.3 Texture evolution

The analysis of pole maps (Fig. 6) and ODF maps (Fig. 7) shows that texture of CP-Ti sheets was significantly affected by annealing temperatures. The texture intensity of CP-Ti sheet annealed at 550 °C was the lowest. The reason was that new oriented equiaxed grains were formed during annealing. With the increase of annealing temperature, the texture intensity of CP-Ti sheets decreased firstly and then increased. The transformation of the basal RD-split texture into basal TD-split texture was affected by the orientation nucleation of recrystallization. More precisely, the texture of annealed sheets transformed from the $(01\bar{1}5)[1\bar{3}21]$ and $(0001)[0\bar{3}31]$ cold-rolled texture into the $(01\bar{1}3)[3\bar{2}\bar{1}0]$ and $(11\bar{2}5)[4\bar{5}10]$ recrystallized texture. Previous studies showed that the typical recrystallized textures of CP-Ti were all basal TD-split textures [22−24]. Generally speaking, there are two main models for the formation of strong and new textures, which are usually described as oriented nucleation or oriented growth [15]. In order to explore the mechanism of texture transformation, the recrystallized grains distribution and pole map of CP-Ti sheet annealed at 550 °C are characterized, as shown in Fig. 9. It can be seen from Fig. 9 that the recrystallized grains had a specific orientation, and the *c*-axis of most recrystallized grains deflected nearly 35° from ND to TD. This was similar to the completely recrystallized texture of CP-Ti sheet annealed at 650 °C, as shown in Fig. 6(d). Therefore, the reason for the transformation of basal RD-split texture into basal TD-split texture was that the recrystallization nucleation of CP-Ti sheets preferentially occurred in the high strain and HAGBs regions. The recrystallized grains had a specific orientation. Moreover, the grain boundaries of these grains had high migration rate and preferential growth, which eventually made the texture transform into a specific direction, and the texture intensity increased slightly.

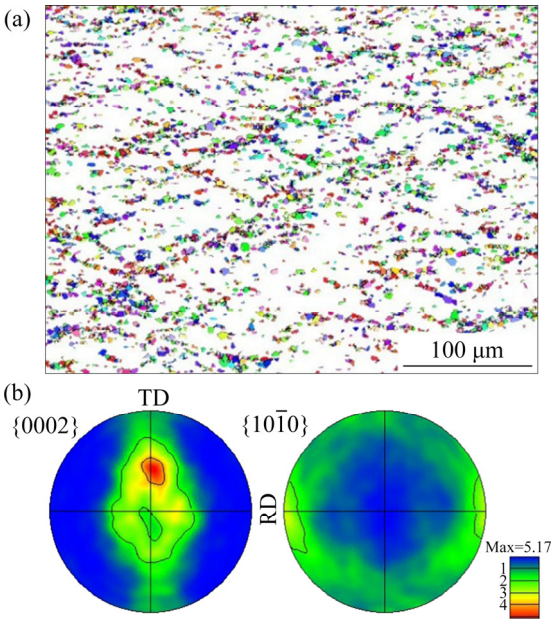

Fig. 9 Recrystallized grains distribution (a) and pole map (b) of CP-Ti sheet annealed at 550 °C

5 Conclusions

(1) When cold-rolled CP-Ti sheet was annealed at 550 °C, the bimodal microstructure could be formed through partial recrystallization, which contributed to obtaining an excellent combination of high strength and good plasticity. The recrystallization rate was 26.7%, and the product of strength and elongation reached 25.6 GPa·%.

(2) The recrystallization nucleation of annealed CP-Ti sheets occurred preferentially in the high strain and HAGBs regions. The internal misorientations of the deformation heterogeneous grains during annealing increased and transformed into HAGBs, which further promoted nucleation of recrystallization.

(3) With the increase of annealing temperature, the texture intensity of annealed sheets decreased

firstly and then increased. The transformation of the basal RD-split texture into basal TD-split texture was affected by the orientation nucleation of recrystallization. The texture of annealed sheets transformed from $(01\bar{1}5)[1\bar{3}21]$ and $(0001)[0\bar{3}31]$ cold-rolled texture into $(01\bar{1}3)[3\bar{2}\bar{1}0]$ and $(11\bar{2}5)[4\bar{5}10]$ recrystallized texture.

Acknowledgments

This work was financially supported by the National Natural Science Foundation of China (No. 52104372), the Fundamental Research Funds for the Central Universities, China (No. N2107001), and the China Postdoctoral Science Foundation (No. 2019M651129).

References

[1] DAI Jing-jie, ZHU Ji-yun, CHEN Chuan-zhong, WENG Fei. High temperature oxidation behavior and research status of modifications on improving high temperature oxidation resistance of titanium alloys and titanium aluminides: A review [J]. Journal of Alloys and Compounds, 2016, 685: 784−798.

[2] WON J W, LEE J H, JEONG J S, CHOI S W, LEE D J, HONG J K, HYUN Y T. High strength and ductility of pure titanium via twin-structure control using cryogenic deformation [J]. Scripta Materialia, 2020, 178: 94−98.

[3] DONG Rui-fei, ZHANG Xiao-yang, KOU Hong-chao, YANG Ling, ZHAO Yu-hong, HOU Hua. Texture evolution associated with the preferential recrystallization during annealing process in a hot-rolled near β titanium alloy [J]. Journal of Materials Research and Technology, 2021, 12: 63−73.

[4] LIU Ding-kai, HUANG Guang-sheng, GONG Gui-lin, WANG Guan-gang, PAN Fu-sheng. Influence of different rolling routes on mechanical anisotropy and formability of commercially pure titanium sheet [J]. Transactions of Nonferrous Metals Society of China, 2017, 27(6): 1306−1312.

[5] ISLAMGALIEV R K, KAZYHANOV V U, SHESTAKOVA L O, SHARAFUTDINOV A V, VALIEV R Z. Microstructure and mechanical properties of titanium (Grade 4) processed by high-pressure torsion [J]. Materials Science and Engineering A, 2008, 493(1/2): 190−194.

[6] MENG Ao, CHEN Xiang, NIE Jin-feng, GU Lei, MAO Qing-zhong, ZHAO Yong-hao. Microstructure evolution and mechanical properties of commercial pure titanium subjected to rotary swaging [J]. Journal of Alloys and Compounds, 2021, 859: 158222.

[7] KANG D H, KIM T W. Mechanical behavior and microstructural evolution of commercially pure titanium in enhanced multi-pass equal channel angular pressing and cold extrusion [J]. Materials & Design, 2010, 31(S1): S54−S60.

[8] NASIRI-ABARBEKOH H, EKRAMI A, ZIAEI-MOAYYED A A, SHOHANI M. Effects of rolling reduction on mechanical properties anisotropy of commercially pure titanium [J]. Materials & Design, 2012, 34: 268−274.

[9] LIU Xiao-min, GAO Hong-liang, WU Hai-jun, PAN Hong-jiang, SHU Bai-po, YANG Yi, LIU Huan, YANG Fei, ZHU Xin-kun. Microstructure and texture characteristics of pure Ti with a superior combination of strength and ductility [J]. Materials Science and Engineering A, 2021, 808(12): 140915.

[10] GU Yan-xia, MA Ai-bin, JIANG Jing-hua, LI Hui-yun, SONG Dan, WU Hao-ran, YUAN Y C. Simultaneously improving mechanical properties and corrosion resistance of pure Ti by continuous ECAP plus short-duration annealing [J]. Materials Characterization, 2018, 138: 38−47.

[11] LI C L, WANG C S, NARAYANA P L, HONG J K, CHOI S W, KIM J H, LEE S W, PARK C H, YEOM J T, MEI Q S. Formation of equiaxed grains in selective laser melted pure titanium during annealing [J]. Journal of Materials Research and Technology, 2021, 11: 301−311.

[12] LIN H K, LI G Y, MORTIER S, BAZARNIK P, HUANG Y, LEWANDOWSKA M, LANGDON T G. Processing of CP-Ti by high-pressure torsion and the effect of surface modification using a post-HPT laser treatment [J]. Journal of Alloys and Compounds, 2019, 784: 653−659.

[13] WANG Yin-min, CHEN Ming-wei, ZHOU Feng-hua, MA En. High tensile ductility in a nanostructured metal [J]. Nature, 2003, 2002, 419(6910): 912−915.

[14] LIN Yong-cheng, TANG Yi, ZHANG Xiao-yong, CHEN Chao, YANG Hui, ZHOU Ke-chao. Effects of solution temperature and cooling rate on microstructure and micro-hardness of a hot compressed Ti−6Al−4V alloy [J]. Vacuum, 2019, 159: 191−199.

[15] DOHERTY R D, HUGHES D A, HUMPHREYS F J, JONAS J J, JENSEN D J, KASSNER M E, KING W E, MCNELLEY T R, MCQUEEN H J, ROLLETT A D. Current issues in recrystallization: A review [J]. Materials Science and Engineering A, 1997, 238(2): 219−274.

[16] LI Jie, NIE Jin-feng, XU Qing-fei, ZHAO Kai, LIU Xiang-fa. Enhanced mechanical properties of a novel heat resistant Al-based composite reinforced by the combination of nano-aluminides and submicron TiN particles [J]. Materials Science and Engineering A, 2020, 770: 138488.

[17] LUNT D, XU X, BUSOLO T, DA FONSECA J Q, PREUSS M. Quantification of strain localisation in a bimodal two-phase titanium alloy [J]. Scripta Materialia, 2018, 145: 45−49.

[18] LI Kai, YANG Ping. Interaction among deformation, recrystallization and phase transformation of TA2 pure titanium during hot compression [J]. Transactions of Nonferrous Metals Society of China, 2016, 26(7): 1863−1870.

[19] CHUN Y B, HWANG S K. Static recrystallization of warm-rolled pure Ti influenced by microstructural inhomogeneity [J]. Acta Materialia, 2008, 56(3): 369−379.

[20] RAY R K, HUTCHINSON W B, DUGGAN B J. A study of the nucleation of recrystallization using HVEM [J]. Acta Metallurgica, 1975, 23(7): 831−840.

[21] HUMPHREYS F J. The nucleation of recrystallization at second phase particles in deformed aluminium [J]. Acta

Metallurgica, 1977, 25(11): 1323−1344.
[22] JIANG Hai-tao, LIU Ji-xiong, MI Zhen-li, ZHAO Ai-min, BI Yan-jun. Texture evolution of commercial pure Ti during cold rolling and recrystallization annealing [J]. International Journal of Minerals, Metallurgy, and Materials, 2012, 19(6): 530−535.
[23] HUANG X S, SUZUKI K, CHINO Y. Improvement of stretch formability of pure titanium sheet by differential speed rolling [J]. Scripta Materialia, 2010, 63(5): 473−476.
[24] LIU N, WANG Y, HE W J, LI J, CHAPUIS A, LUAN B F, LIU Q. Microstructure and textural evolution during cold rolling and annealing of commercially pure titanium sheet [J]. Transactions of Nonferrous Metals Society of China, 2018, 28(6): 1123−1131.

退火温度对冷轧商业纯钛板材组织和力学性能的影响

赵 帅[1], 王 洋[1], 彭 琳[1,2], 张元祥[1], 冉 蓉[1], 袁 国[1]

1. 东北大学 轧制技术及连轧自动化国家重点实验室，沈阳 110819；
2. 攀钢集团研究院有限公司，攀枝花 617067

摘 要：传统的商业纯钛(CP-Ti)合金强度往往不能满足结构材料的需求。为了提高其力学性能，对冷轧 CP-Ti 合金在不同温度下退火，并详细研究其再结晶行为和织构演变。结果表明，部分再结晶形成的双态结构(等轴和拉长的晶粒)表现出极限抗拉强度(702 MPa)和总伸长率(36.4%)的优异结合。CP-Ti 板材的再结晶形核优先发生在高应变和大角度晶界区域。同时，变形不均匀晶粒的内部取向差增大并转变成大角度晶界，进一步促进再结晶形核。主要再结晶织构是由冷轧基面 RD-分裂织构转变而来的基面 TD-分裂织构，再结晶过程中定向形核起主导作用。

关键词：商业纯钛；再结晶形核；双态组织；力学性能；织构

(Edited by Xiang-qun LI)